Chemistry Europe
European Chemical Societies Publishing

Special Collection

The Dependence of Chemical Quantum Yields of Visible Light Photoredox Catalysis on the Irradiation Power

Barbara Reiß,[a] Qi Hu,[b] Eberhard Riedle,*[b] and Hans-Achim Wagenknecht*[a]

Despite the great achievements of advanced photoredox catalysis for organic-synthetic reactions, the literature is rather vague with respect to reaction quantum yields – the number of product molecules per absorbed photon. This stands in contrast to the clear and commonly used chemical yield as standard parameter to quantify the efficiency of chemical reactions. We applied an opto-electronic device to measure the reaction quantum yields of a reference reaction in a rapid and facile way, which revealed that this parameter cannot be regarded as a single, isolated value. A so far undescribed strong dependence of the reaction quantum yield on the incident light power and the irradiation time was revealed. The light input even decides on the interplay of the closed photoredox catalytic cycle and the radical chain propagation. The reaction kinetics were modelled in full detail to obtain important insight into the general description of photoredox catalytic mechanisms.

1. Introduction

Chemical photocatalysis links the physical process of light absorption and excitation of a recycled catalyst to desired chemical reactions. The challenge to use low energy photons corresponding to visible light instead of UV light commonly applied for this type of photochemistry, has been solved by applying photoinduced electron transfer reactions instead of energy transfer processes to initiate chemical reactions. This approach was named photoredox catalysis, a research field that has been established over the past decade.[1–19] Sunlight as an essentially unlimited and thereby "green" natural light source or LEDs as cheap and energy-saving artificial sources for controlled irradiation in pilot investigations can be applied for sustainable chemical photocatalysis.

Transition metal complexes and organic dyes are commonly used as photocatalysts. The current "working horse" for photoredox catalysis is Ruthenium tris(bipyridine) – $[Ru(bpy)_3]^{2+}$,[20] due to its strong MLCT absorption, the long living triplet state, the versatile redox behavior (Ru^{3+} vs. Ru^{+}) and the chemical and photochemical robustness. Moreover, organic compounds like flavin,[21,22] rhodamine 6G,[23] 9-mesityl-10-methylacridiniumperchlorat,[24] 1,2,3,5-tetrakis(carbazol-9-yl)-4,6-dicyanobenzenes[25] and N-phenyl phenothiazines[26] were evaluated to further strengthen the sustainability of chemical photocatalysis by avoiding transition metal complexes.[27,28] The current literature about chemical photocatalysis describes achievements for advanced and complex organic-chemical reactions. However, it is rather vague or even inaccurate with respect to the determination of the photo efficiency – the number of product molecules per absorbed photon – and rather the chemical yield after a convenient reaction time is reported. Detailed knowledge of the mechanistic intricacies is fundamental to fruitfully pursue future research on photoredox catalysis which might be the reason why mechanistic investigations represent a considerable share of current publications on the topic.[15] The early focus on synthetic feasibility leaves us today with a great challenge to compare and assess the performance of different photoredox catalysts as a multitude of different (each optimized) conditions were applied in precedent experiments.

First of all, a lot of different light sources are used, ranging from Hg/Xe lamps, compact fluorescence lamps (CFLs), to LEDs and others. They vary largely not only in the emission spectrum but also in the optical output power. Secondly, it is many times not even clearly reported, how the absorption spectrum of the catalyst and the lamp spectrum overlap or whether the substrate already reduces the useable optical power by direct absorption. Thirdly, the reaction quantum yield is determined mainly by chemical actinometry that was standardized by IUPAC.[29] Although chemical actinometry can be done with special instrumentation other than an absorbance spectrometer, it is rather laborious and error-prone, since it relies on only a few reference values for standard compounds measured to a major part in the 60s and 70s of the last century. These probably are the reasons, why – in contrast to the clear and commonly used chemical yield as standard parameter to describe and quantify the efficiency of chemical reactions (organic or inorganic) – the reaction quantum yield is still not

[a] Dr. B. Reiß, Prof. Dr. H.-A. Wagenknecht
Institute of Organic Chemistry
Karlsruhe Institute of Technology (KIT)
Fritz-Haber-Weg 6, 76131 Karlsruhe (Germany)
E-mail: Wagenknecht@kit.edu
[b] Dr. Q. Hu, Prof. Dr. E. Riedle
Lehrstuhl für BioMolekulare Optik
Ludwig-Maximilians-Universität (LMU)
Oettingenstraße 67, 80538 München (Germany)
E-mail: Riedle@physik.uni-muenchen.de

Supporting information for this article is available on the WWW under https://doi.org/10.1002/cptc.202100090

Special Collection An invited contribution to the "GDCh and ChemPhotoChem: 5-Year Anniversary" Special Collection

routinely determined. This is astonishing since reaction quantum yields are a crucial experimental result to distinguish between photoredox catalytic reactions and photocatalytically induced chain reactions.[30,31] It makes clear, that the accurate reaction quantum yield is a highly valuable parameter to normalize and reference the performance of different photocatalysts and reactions.

A novel opto-electronic device allows the direct and facile determination of absolute reaction quantum yields in a typical organic-chemistry laboratory.[32] The apparatus relies on high-power LEDs as light source and not on literature reference values, but on the quantitative determination of the light input, the absorbed amount of light and the amount of product over the time course of an organic-chemical photocatalysis. In detail, we image the millimeter size emission area of high power LEDs with suitable high numerical aperture optics into the sample. The strength of illumination can be changed at will by the drive current of the LED and/or additional optical filters. Practically any excitation wavelength from the UV–C to the NIR can be chosen by the proper LED. The sample is placed in spectroscopic cuvettes of high optical quality to ensure that no measured light misses the sample and the transmitted light can be measured precisely to determine the actually absorbed amount. The use of the spectroscopic cuvette might seem like a practical disadvantage as it has to be cleaned for each run, but this is much less time consuming and critical than all the other steps in a typical synthetic workflow. In this work, we establish this direct determination of the reaction quantum yield on a well-known photoredox catalyzed reaction, which elucidates a so far undescribed dependence of the reaction quantum yield on the incident light power and the irradiation time, and gives important insights into the general description of photoredox catalytic mechanisms.

2. Results and Discussion

2.1. Methodology and Reference Reaction

Based on the general IUPAC definition for any radiation-induced process,[29] the reaction quantum yield Φ for a given product of a photochemical or photocatalytic reaction is defined as Equation (1):

$$\Phi = \frac{\text{number of product formed}}{\text{number of photons absorbed}} = \frac{N_{product}}{N_{photon}} \tag{1}$$

Accordingly, the determination of the reaction quantum yield requires both the ability to measure the number of product molecules formed and the ability to quantify the number of photons absorbed. The first parameter, the chemical yield, can be determined by established methods, mainly balance weight of isolated and pure compounds (with respect to the molecular weight) or spectrometric analysis of reaction mixtures, such as NMR and GC.

The simple definition of the quantum yield has some intrinsic problems. Firstly, the irradiation time is not explicitly included by the IUPAC description.[33] Secondly, if the reaction is driven by a constant light input well beyond the completion of the synthesis, the value Φ will asymptotically decrease to 0. So we distinguish the following quantities in this work [Eq. (2)]:

$$\Phi_{tot} = \frac{N_{product}(t = t_{syn})}{N_{photon}(t = t_{syn})} \tag{2}$$

with t_{syn} the total time of the light driven synthesis. This is a quantity that – in the best scenario – is minimized by the chemist or purely determined by the work hours. When we investigate the illumination time dependence of Φ_{tot} (see below), we can determine the maximum value of Φ_{tot} [Eq. (3)]

$$\Phi_{max} = \max_{t_{syn}}(\Phi_{tot}) \tag{3}$$

This gives the best usage of the photons neglecting the wish to optimally use the substrates and any other chemicals used in the synthesis. One can readily derive from measured data that Φ_{max} is not necessarily found for the very beginning of the synthesis as would be expected for the simplest possible photocatalytic processes. Instead many reactions need a certain initiation or induction phase to really make use of the illumination. Therefore the intrinsic ability to utilize the photons is given by the time dependent differential quotient [Eq. (4)][33]

$$\Phi_{diff}(t) = \frac{\Delta N_{product}(t)}{\Delta N_{photon}(t)} \tag{4}$$

where $\Delta N_{product}$ is the increase in product over a small interval Δt and ΔN_{photon} the number of absorbed photons during that interval. Technically, we determine the differential quantum yield Φ_{diff} by finite difference quotients.

The above described method to determine the reaction quantum yield applies also for the reference reaction of this study which was the α-alkylation of 1-octanal (**Oct**) by 2-bromo-diethylmalonate (**BrMal**) yielding the product diethyl (*R*)-2-(1-oxooctan-2-yl)malonate (**DOM**) (see Scheme 1).[34] [Ru(bpy)$_3$]Cl$_2$ (**Ru**) was applied as photoredox catalyst together with the chiral imidazolidinone (**OrCat**) as organocatalyst to achieve enantioselectivity. We chose this reaction because (i) it is an important benchmark reaction that can be photocatalyzed by a variety of different photoredox catalysts, and (ii) it is one of the few reactions with values of the reaction quantum yield reported. Furthermore, (iii) the chemical yield can easily be determined by NMR with reference to diethyl bromomalonate. The molar absorption coefficient of all catalysts and substrates are summarized in Figure 1 together with the emission spectrum of the 432 nm LED. It can be seen that only the Ru catalyst absorbs the LED light.

Remarkably, the published reaction quantum yield for this reaction varies from $\Phi = 0.49$ (Table 1, line 1)[32] to $\Phi = 18$ (Table 1, line 2).[30] This is a critical issue since reaction quantum yields higher than 1 require a chain propagation mechanism that significantly alters the mechanistic scenario of a photocatalytic reaction (Figure 2).[30,31] The reactions were performed

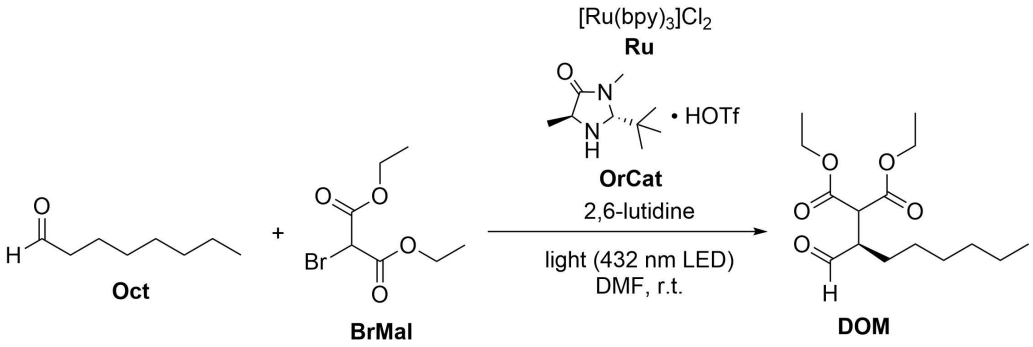

Scheme 1. Photocatalytic and enantioselective α-alkylation of 1-octanal (**Oct**): 1.00 M **Oct**, 500 mM **BrMal**, 2.50 mM $[Ru(bpy)_3]Cl_2$ (**Ru**), 100 mM organocatalyst (**OrCat**), 1 M 2,6-lutidine in 1.3 mL DMF, stirring at r.t. The initial concentrations of **Oct**, **BrMal**, **Ru** and **OrCat** are matched to the literature and were always the same in our photocatalytic experiments.

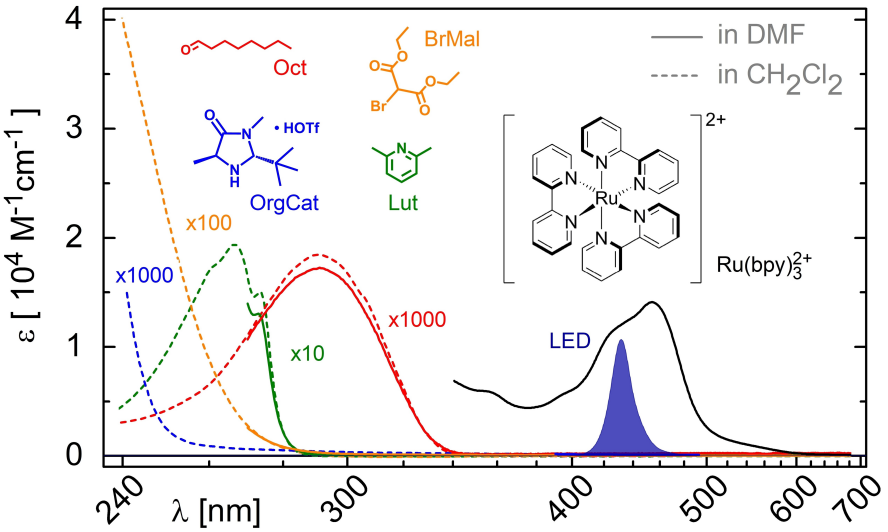

Figure 1. Steady-state absorption spectra of **Ru** and the reactants for α-alkylation of **Oct** in CH_2Cl_2 or DMF at room temperature. The royal blue filled curve represents the emission of the LED.

Table 1. Reported reaction quantum yields of the photoredox organocatalytic α-alkylation of octanal (**Oct**) by 2-bromomalonic dieethylester (**BrMal**) (see Scheme 1).

Line	Catalyst[a]	Light source	Irradiation time	Yield [%]	Φ	Ref.
1	$[Ru(bpy)_3]Cl_2$	20.5 mW 443 nm LED[b]	1 h	14	0.49	[32]
			2 h	27	0.47	
			3 h	36	0.42	
2	$[Ru(bpy)_3]Cl_2$	spectrofluorimeter 436 nm (slit 10 nm) 184 μW[c]	4 h	27	18[d]	[30]
3	direct excitation of enamine	300 W Xe lamp[e] with bandpass filter @ 400 nm, 120 μW	16	95	20[d]	[39]
4	Eosin Y	1 W 530 nm LED[e]	6 h	19	0.09	[35]
5	$[Ru(bpy)_3]Cl_2$	28.3 mW 432 nm LED[b]	1 h	56	0.95[d]	This work
			2 h	74	0.63[d]	
			3 h	80	0.45[d]	

[a] Catalyst loading 0.5 mol%. [b] Irradiation determined at the sample. [c] Calculated irradiation output from photon flux (see the Supporting Information). [d] Determined based on potassium ferrioxalate chemical actinometry.[37] [e] Electric power used to drive the light source.

under very similar conditions. However, the only obvious and neglected difference between the two experimental setups was the applied power of the light sources. It differs by two orders of magnitude, i.e. 20.5 mW for the 443 nm LED[32] and 184 μW for the bandwidth restricted spectrofluorimeter as light source.[30] In direct comparison, the published reaction quantum yield of 18[30] seems to be extraordinarily high, not only with respect to the usage of $[Ru(bpy)_3]^{2+}$ but also eosin Y as photocatalysts ($\Phi = 0.09$, line 3).[35] Direct excitation of the charge-transfer complex formed with a very electron-deficient

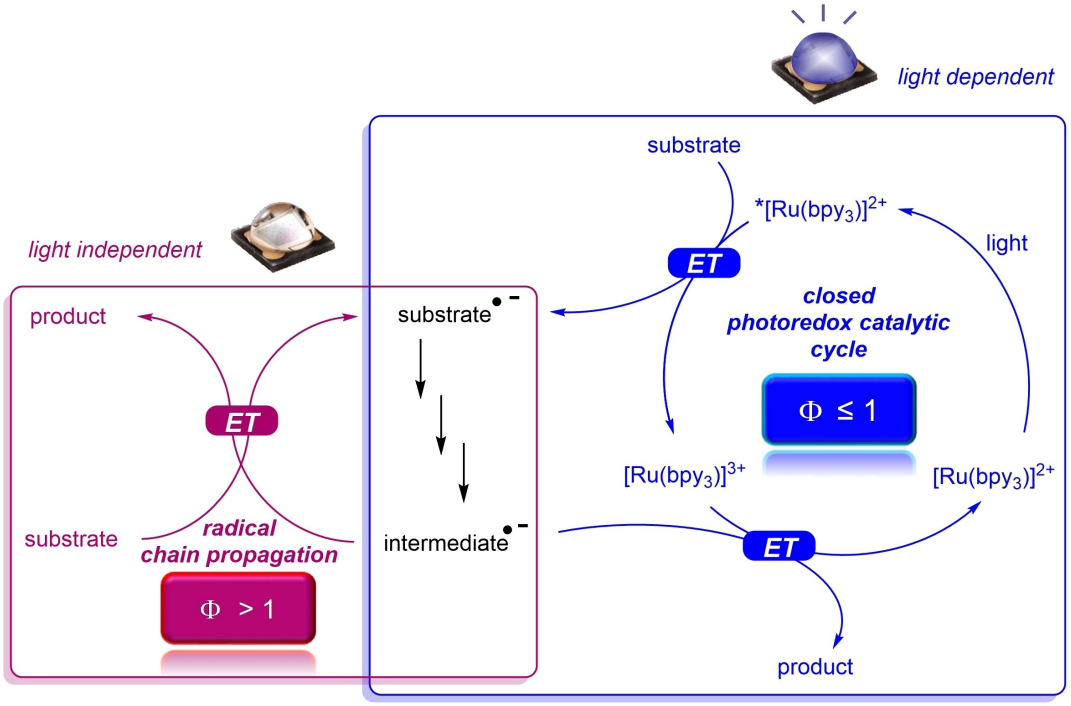

Figure 2. The light-dependent, closed photoredox catalytic cycle (blue) is characterized by $\Phi \leq 1$, the radical chain propagation (purple) causes $\Phi > 1$. For the latter light-independent process, light is only needed for initiation (see Scheme 2).

organocatalyst renders the photocatalyst and gives a reaction quantum yield of 20.[39] The main aim of this work is to investigate and reveal the connection between the illumination strength, the underlying reaction mechanism and the resulting values of the reaction quantum yield.

For the measurement of the amount of photons it is important to distinguish between the incident photon flux or light power P_{irr} and the absorbed photons or absorbed light power P_{abs} that induce the chemical reaction. The two quantities are related by the absorption of the sample and a small correction due to the reflection off the cell windows.[32] In the present investigation the absorbance of the Ru catalyst is 32 and therefore all impinging blue light is absorbed. The only correction needed for the determination of the absorbed light is the reflectivity of the cuvette windows. Our physical device, as mentioned above, can be considered as "direct" actinometer because it converts the amount of incident or transmitted photons into a quantifiable electrical signal. On the other hand, the indirect chemical actinometry is widely applied since the amount of molecules that reacted is believed to be conveniently determined by UV/Vis absorption spectroscopy.[29,36,37] Together with literature-known reference values, the actinometer allows to determine the photon flux and thus the number of photons absorbed by the substrates.

Our device for direct determination of reaction quantum yields was calibrated for the described photocatalytic α-alkylation by the ferrioxalate actinometer (see Supporting Information) at different irradiation times (1 h, 2 h, 3 h) and an incident light power of 28.3 mW at 432 nm. The deviations from the earlier results[32] are rather small ($\Phi = 0.42$ vs. 0.45 after 3 h irradiation) and believed to be within the experimental error. It thus becomes clear that the chemical actinometry can be replaced by the opto-electronic device that allows not only the facile but also the exact and validated determination of reaction quantum yields during the time course of this photocatalytic reaction.[32,38]

Our quantum yield determination device was upgraded in many ways since the original publication.[32,38] We extended the selection of LEDs largely and cover now the full range from 255 nm to above 1000 nm without gaps. At the same time the maximum output power of the LEDs was increased. To collect even more light, the photographic lens was replaced by either fused silica best form lenses or an aspheric lens in combination with a 2" diameter spherical lens with about a factor of 5 higher collection efficiency. An electromagnetic shutter was added to allow the control of the illumination with sub-0.1 s precision and no need to open the setup enclosure. For the use of deaerated samples the casing was expanded (see Figure S5). Finally, the original solar cell optimized for visible light was replaced with an uncoated large area solar cell that is highly sensitive even in the UV–C. To precisely determine the irradiation, we now measure the light induced current directly be either a suitable multimeter or a current-to-voltage converter of our own design based on a published high sensitivity design with a huge dynamic range.[40] By variation of the LED drive current and additional neutral density filters the light power at the sample can be varied continuously over more than 3 orders of magnitude. In order to elucidate the assumed influence of the applied light sources, in particular their powers and energies, which could possibly account for the capital

disparity of determined quantum yields Φ, we determined both the chemical yield and Φ in a time-dependent way using our device at a range of low to medium light powers (30 μW to 10 mW). Aliquots were taken to determine the chemical yield via NMR spectroscopy over the course of the reaction to trace the temporal progression of the formation of **DOM**.

2.2. Experimental Results

The result of the irradiation of the reaction with the varying light power impinging on the sample is shown in Figure 3. We measured the chemical yield after selected irradiation times up to 72 hr. Preliminary experiments showed that even after a day the reaction was not yet complete for the weaker illumination levels that are needed to highlight the radical chain mechanism. For some of the illumination levels the experiment was only performed up to 24 hr to save experimental time. There is a monotonic increase of product concentration with time up to near saturation. But is it also readily seen, that the illumination level has a profound impact. At first glance, the chemical yield of **DOM** does show the expected dependence on the light input (Figure 3, a and b). The product formation at lower light input powers works as expected with lower effective rates and final yields. For very low irradiation powers (500 μW and lower) there is an obvious induction period until the process of product formation turns to its optimal efficiency under the applied conditions. This induction phase could be attributed to the inefficient enamine formation between substrate **Oct** and the organocatalyst **OrCat**. This fits the description in the literature that the formation of the enamine **Ena** is unfavorable and described by a low equilibrium constant ($K_{eq} = 8.1 \cdot 10^{-3}$).[30,39] In addition, any trace impurities that initially hinder the product formation, could be used up by secondary photo processes.

The photoredox reaction is initiated (see Scheme 2) by the electron transfer between photoexcited $*[Ru(bpy)_3]^{2+}$ and enamine **Ena** that produces not only the enamine radical cation $\mathbf{Ena}^{+\bullet}$ but also – after back electron transfer to the ruthenium complex – the malonate radical $\mathbf{Mal}^{\bullet}$ that plays a crucial role in the catalytic cycle (see below).[30] The following period of quite rapid and constant product formation is clearly non-proportional with regards to the incident light power. At longer irradiation times (over up to 5 h) the conversion of **Oct** shows a nearly linear further increase of the chemical yield. At low irradiation powers, however, the chemical conversion of **Oct** to **DOM** does not get completed because the organocatalyst **OrCat** gets destroyed over longer irradiation time. Due to the crucial role of **Ena** for the induction of the photoredox catalysis and the fact that a reduced **OrCat** concentration immediately

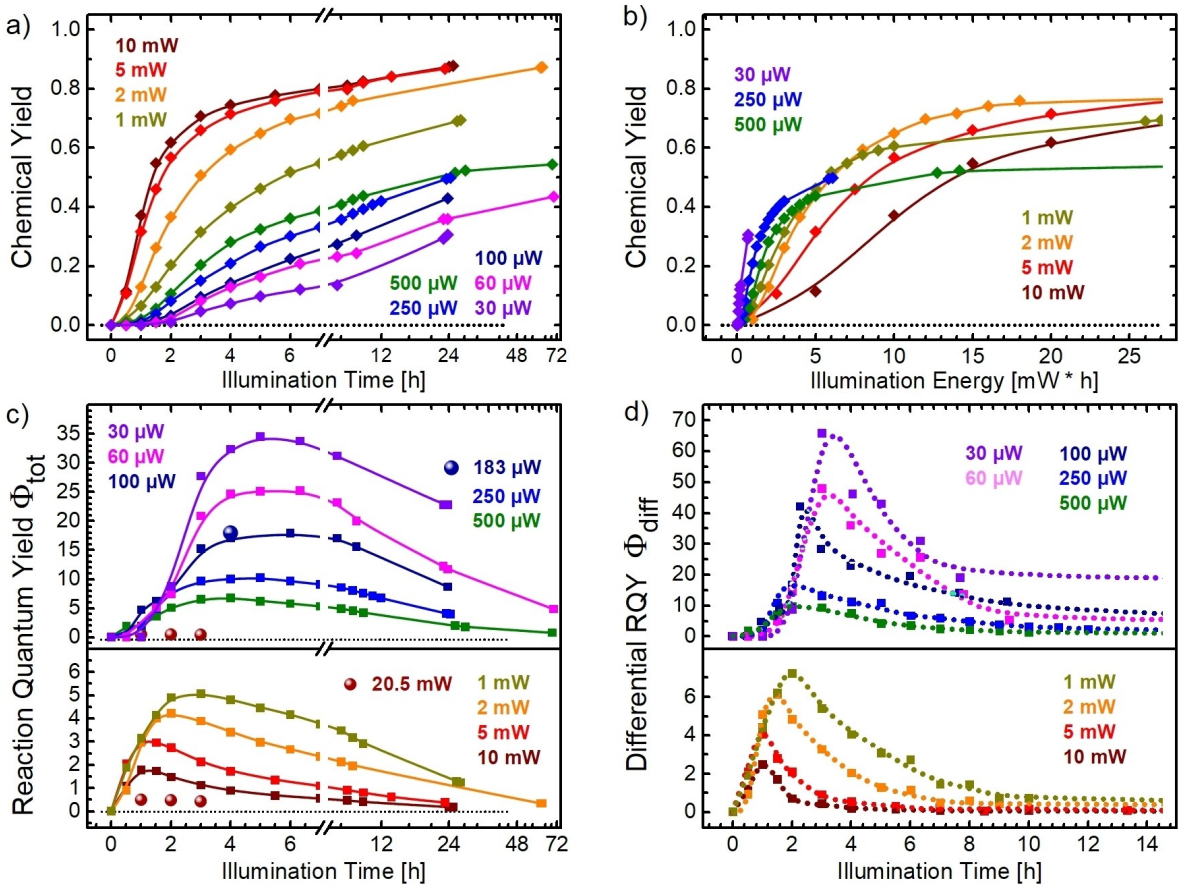

Figure 3. a) Time-dependent and b) energy-dependent chemical yield, and c) total (Φ_{tot}) and d) differential reaction quantum yield (Φ_{diff}) for the photocatalytic conversion of **Oct** and **BrMal** to the **DOM** at various excitation powers (30 μW–10 mW). The lines in (d) are "guides to the eye".

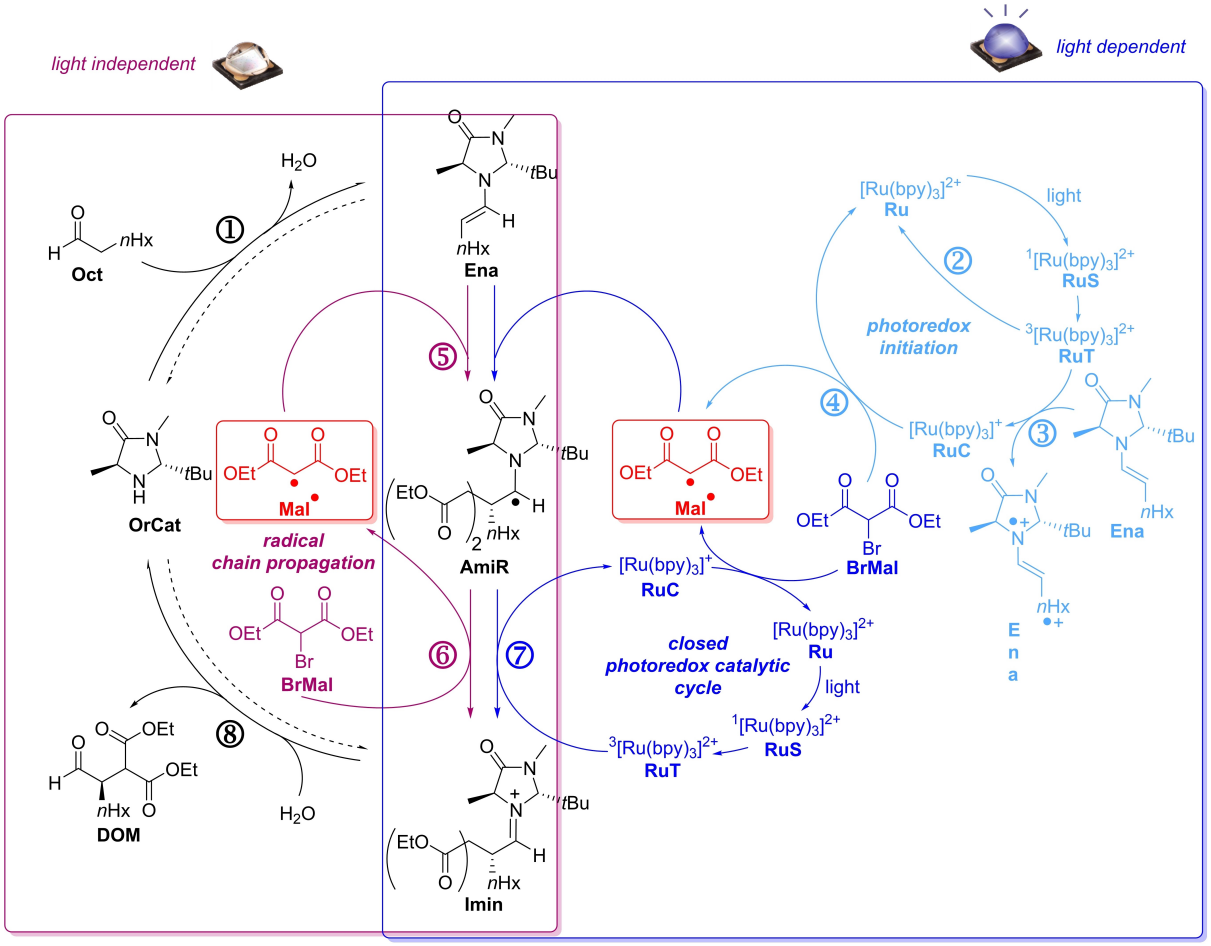

Scheme 2. Coupled mechanisms consisting of photoredox catalytic cycle (blue) and radical chain propagation (purple). The central malonate radical **Mal**$^{\bullet}$ links both scenarios and competes between both mechanisms. The organocatalytic cycle (black) is involved in both radical mechanisms promoting enantioselectivity. The photoredox initiation cycle (light blue) oxidizes the enamine **Ena** by electron transfer to the radical cation **Ena**$^{+\bullet}$ and back electron transfer to the substrate. **BrMal** yields the most important malonate radical **Mal**$^{\bullet}$.

reduces the **Ena** concentration, more photoinitiation cycles are needed. At higher irradiation powers, the reactions are completed before the organocatalyst **OrCat** is destroyed.

In Figure 3 b) the chemical yield is plotted as a function of the integrated illumination energy. According to the most simple picture of a chemical photocatalysis, the total absorbed energy or number of photons determines the product formation. Clearly this expectation fails and dramatically different yields results for the same absorbed photon number under different illumination levels. From the measured chemical yield at selected times and absorbed light power we calculate the reaction quantum yield Φ_{tot} according to Equation (2) (see Figure 3 c). Now it becomes even clearer that the investigated processes depend extremely strongly both on time and light level. The maximum value of 35 – please note that this is not %, but a large factor – points directly to a chain propagation. Finally, we can derive the differential reaction quantum yield Φ_{diff} (see Figure 3d). Here the maximum value increases up to 65 as the integral values of Φ_{tot} have already averaged over the slow induction period and the following phase of maximum conversion speed.

2.3. Qualitative Discussion

For the discussion of the reaction quantum yield Φ it firstly became obvious that Φ must be considered as a function of time (Figures 3c) and 3d)). Mainly due to substrate conversion and possibly catalyst degradation, the quantum yield Φ_{tot} drops over longer irradiation times. As we most likely consider diffusive processes, the decreased substrate concentration leads directly to a lower conversion efficiency. Our values agree well with reported reaction quantum yields, which are in particular $\Phi_{tot} = 0.42$ for 20.5 mW and $\Phi_{tot} = 18$ for 184 µW incident light power, respectively (Table 1 and inset spots in Figure 3c)). It became clear, however, that these reported reaction quantum yields must be considered as single snapshots at given irradiation times. Correctly speaking, they are the averages over the illumination time up to the moment when the chemical yield is determined (Figure 3c)). The results make clear that the reaction quantum yield cannot be viewed as a single, isolated value but must be considered not only as a function of irradiation time but also of incident light power.

The maximum Φ_{max} is found to be proportional to the reciprocal square root of the irradiation power (Figure 4). A similar dependence was observed for a photoinduced radical chain mechanism.[41] Also early theoretical considerations predict such a behavior in a related situation.[42] To our knowledge, this was never taken into account for photoredox catalysis, and is best reflected by the differential reaction quantum yield Φ_{diff} which was determined numerically from the data at individual time steps. Secondly and most importantly, both reaction quantum yields, Φ_{tot} and Φ_{diff}, determined at incident light powers lower than 20 mW are all above 1 which means that every photon absorbed gives clearly more than one molecule of the product **DOM**. In fact, the maximum values of the quantum yield $\Phi_{tot} = 25$ and 35 were determined for 60 μW and 30 μW incident light power, the lowest in our measurements, each after 5 h irradiation (Figure 3).

The observations clearly show that the power of the incident light exerts a decisive influence on the proceeding mechanism of the photo-initiated reaction, in particular between a faster operating open-shell chain propagation mechanism for low light input and a shift towards a closed photocatalytic cycle mechanism for high light input (Scheme 2). The existence and evidence of both mechanisms is still a current topic of debate.[30,31] The crucial parameter that decides between the two mechanisms is the occurrence of the radical **Mal•**. This is the relay and key intermediate formed from **BrMal** by one-electron reduction and consumed by **Ena** quenching. Higher concentrations of $*[Ru(bpy)_3]^{2+}$ at higher irradiation powers suggest a preferential quenching of enamine **Ena** by the photoredox formed radical **Mal•** in a tightly closed catalytic cycle. This reduces the maximum quantum yields Φ_{max}. In contrast, higher steady-state concentrations or even excess of the radical **Mal•** result(s) in a favored enamine **Ena** quenching by this intermediate. Eventually too high concentrations of **Mal•** will result in unidentified side reactions that limit the **Mal•** concentration. This is considered by the rate k_9 in our model (see below). The described situation decouples the photocatalytic production of **Mal** from the organocatalytic reaction by the chain propagation mechanism. Since the latter process is light-independent, reaction quantum yields significantly higher than $\Phi = 1$ are achieved. The occurrence of the two different product-forming mechanisms can be controlled by the incident light and are controlled by the steady-state concentration (modelled in the simulations, see below) of the radical **Mal•** as relay between both mechanisms.

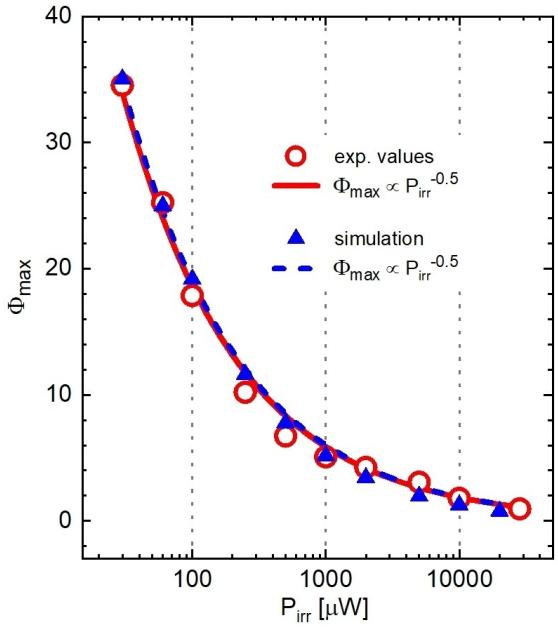

Figure 4. The maximum reaction quantum yield Φ_{max} is found to be proportional to the reciprocal square root of the incident light power. This is seen both in the experiment and the simulation (see below).

Due to its extremely short life time, the **Mal•** is not directly observable for us. We therefore resorted to the method of intermittent illumination that was developed in the middle of the last century to investigate radical chain reactions.[43,44] Briefly, the light driving the reaction is periodically interrupted – classically by a chopper – and the rate varied. If the period of chopping is short compared to the life time of a chain, no difference to a continuous illumination results. However, when the chain comes to termination before the next light pulse and the steady-state radical concentration is not reached in the on-period, a reduced reaction yield results for constant average illumination power. This method, also termed rotating sector method, has recently been transferred to LED irradiation[45] and with a pulsing circuit of our own design we can realize on/off cycles as short as 10 μs.[38]

We performed a series of illuminations with the same chemical composition of the sample as in the other measurements. A ratio of 9:1 was chosen for the light off to on periods. In this way the sample has optimum time to relax in each illumination cycle, i.e. the radical concentration can decrease due to the unidentified termination reaction. This has already been pointed out in literature,[44] where it is concluded that "dispersion is increased" for larger values of the off/on ratio. At the time, the classical light sources and mechanical choppers did not allow this, but with our electronic pulser it can readily be achieved.

From the evaluation of the measured data according to Shepp[44] we obtain a value of the temporal chain length of 23 μs (for details see SI). If we now take the highest values for the reaction quantum yield of a few tens as a measure of the number of steps taken by the average chain, we can derive a step size of just below 1 μs for the chain reaction. This seems quite reasonable for the high concentration of **BrMal** and **Ena** and diffusion conditions. Finally, we can combine this information with the highest illumination of 10 mW to derive a concentration of **Mal•** of only 500 pM. This seems extremely small, but due to the large excess of all other reagents the μs reaction time in the chain outweighs the low concentration and the overall process becomes quite effective for the many hours of synthesis.

2.4. Quantitative Simulation

To simulate the light intensity-dependent dynamics, we developed a mathematical model that describes our new proposed mechanism. In essence, this is simply a rate model with the illumination modelled by the volumetric rate of light absorption $\tilde{J}_{abs}$ ((moles of photons)·L^{-1}·s^{-1}), i.e. a time-dependent "concentration" input of light, to be compatible with other terms, i.e. concentrations and rates [Eq. (5)].

$$\tilde{J}_{abs} = P_{abs} \cdot \frac{\lambda}{h \cdot c} \cdot \frac{1}{N_A} \cdot \frac{1}{V} \tag{5}$$

P_{abs} is the absorbed light power that is derived from the irradiation power P_{irr} and the sample absorption, λ the center wavelength of the light source and V the solution volume. h, c and NA are the Planck constant, the speed of light in air and the Avogadro constant, respectively.

We assume a quasi-equilibrium distribution inside the reaction cuvette that is only partially illuminated but rapidly stirred. Alternatively one can consider the rate constants as effective values. The time dependence of the respective concentration of each chemical substance (see Scheme 2 for the naming) is described by Equations (6):

$$\frac{d[\mathrm{OrCat}]}{dt} = -k_1[\mathrm{OrCat}][\mathrm{Oct}] + k_{-1}[\mathrm{Ena}][H_2O] + k_8[\mathrm{Imin}][H_2O] - k_{-8}[\mathrm{DOM}][\mathrm{OrCat}] \tag{6.1}$$

$$\frac{d[\mathrm{Oct}]}{dt} = -k_1[\mathrm{OrCat}][\mathrm{Oct}] + k_{-1}[\mathrm{Ena}][H_2O] \tag{6.2}$$

$$\frac{d[H_2O]}{dt} = k_1[\mathrm{OrCat}][\mathrm{Oct}] - k_{-1}[\mathrm{Ena}][H_2O] - k_8[\mathrm{Imin}][H_2O] + k_{-8}[\mathrm{DOM}][\mathrm{OrCat}] \tag{6.3}$$

$$\frac{d[\mathrm{Ena}]}{dt} = k_1[\mathrm{OrCat}][\mathrm{Oct}] - k_{-1}[\mathrm{Ena}][H_2O] - k_3[\mathrm{Ena}][\mathrm{RuT}] - k_5[\mathrm{Ena}][\mathrm{Mal}] \tag{6.4}$$

$$\frac{d[\mathrm{Ru}]}{dt} = -\tilde{J}_{abs} + k_2[\mathrm{RuT}] + k_4[\mathrm{RuC}][\mathrm{BrMal}] \tag{6.5}$$

$$\frac{d[\mathrm{BrMal}]}{dt} = -k_4[\mathrm{RuC}][\mathrm{BrMal}] - k_6[\mathrm{AmiR}][\mathrm{BrMal}] \tag{6.6}$$

$$\frac{d[\mathrm{RuT}]}{dt} = \tilde{J}_{abs} - k_2[\mathrm{RuT}] - k_3[\mathrm{Ena}][\mathrm{RuT}] - k_7[\mathrm{AmiR}][\mathrm{RuT}] \tag{6.7}$$

$$\frac{d[\mathrm{RuC}]}{dt} = k_3[\mathrm{Ena}][\mathrm{RuT}] - k_4[\mathrm{RuC}][\mathrm{BrMal}] + k_7[\mathrm{AmiR}][\mathrm{RuT}] \tag{6.8}$$

$$\frac{d[\mathrm{Mal}]}{dt} = k_4[\mathrm{RuC}][\mathrm{BrMal}] - k_5[\mathrm{Ena}][\mathrm{Mal}] + k_6[\mathrm{AmiR}][\mathrm{BrMal}] - k_9[\mathrm{Mal}] \tag{6.9}$$

$$\frac{d[\mathrm{AmiR}]}{dt} = k_5[\mathrm{Ena}][\mathrm{Mal}] - k_6[\mathrm{AmiR}][\mathrm{BrMal}] - k_7[\mathrm{AmiR}][\mathrm{RuT}] \tag{6.10}$$

$$\frac{d[\mathrm{Imin}]}{dt} = k_6[\mathrm{AmiR}][\mathrm{BrMal}] + k_7[\mathrm{AmiR}][\mathrm{RuT}] - k_8[\mathrm{Imin}][H_2O] + k_{-8}[\mathrm{DOM}][\mathrm{OrCat}] \tag{6.11}$$

$$\frac{d[\mathrm{DOM}]}{dt} = k_8[\mathrm{Imin}][H_2O] - k_{-8}[\mathrm{DOM}][\mathrm{OrCat}] \tag{6.12}$$

This model does the exact book keeping for the usual chemical description shown in Scheme 2. In particular, the multiple appearances of some of the substances and the possible reversible processes are completely described in this way. A weak loss channel leading to an unidentified side product has been included in Equation (6.9) with the term "-k_9 [Mal]". As an example consider Equation (6.7). Light absorption is only possible under our conditions by the catalyst **Ru**. Each absorbed photon transfers a molecule **Ru** to **RuS** (excited single state). As the ISC from **RuS** to **RuT** (excited triplet state) is practically unity, we do not have to consider **RuS** explicitly, but operate immediately with **RuT**. Now there are two paths for **RuT** to be used up: either the encounter with **Ena** to render **RuC** and the radical cation **Ena**$^{+\bullet}$, or the encounter with the radical **AmiR** to render again **RuC** and **Imin**. Therefore the change in **RuT** concentration is equal to the absorbed photon rate $\tilde{J}_{abs}$ minus the respective rate for the depletion processes times the product of the encounter pair concentrations. Finally, there is a finite probability that the excited triplet state decays to the ground state by photophysical processes rather than the photochemical reactions (with **Ena**$^{+\bullet}$ or **AmiR**). This is considered as rate k_2, For the convenience of the reader the numbering of the rates is indicated in Scheme 2 for all forward reactions with the rate index circled. As we have to consider many of the processes as reversible, there are many matching rates k_{-i} to the forward rate k_i.

The model is highly nonlinear so that it is unlikely to possess a closed-form solution. Therefore, there are obvious difficulties in fitting all the rate constants of the reactions in a global fit. Fortunately, some rate constants have been reported in the literature. The rest of them are inferred reasonably based on the steady-state assumption or based on the diffusion

limited rate constant. The complete list of the applied rate constants is given in Table 2. A simple example is the association of the **Ena** as the association constant has been reported to be $K_{eq} = 8.1 \times 10^{-3}$.[30] Inspection of Scheme 2 immediately renders $K_{eq} = k_1/k_{-1}$. The loss rate k_3 of the **Ena** certainly has to be much smaller than the production rate k_5. The latter can at best be diffusion limited. For a full account on the estimation of the rate constants, please refer to ref.,[46] chapter 3. The final optimization was done by visual inspection of a good simultaneous match with the experimental data for all illumination levels. As we developed a deep understanding which constants preferentially change which observables, a surprisingly fast "convergence" was found.

Based on the uniform initial concentrations in our quantum yield experiments, we can employ the model to calculate time- and light intensity dependent concentration profiles for the product **DOM**. Finally, the reaction quantum yield Φ_{tot} is computed by Equation (7):

$$\Phi_{tot}(t) = \frac{[\mathbf{DOM}](t)}{t} \cdot \frac{1}{\tilde{J}_{abs}} \quad (7)$$

The simulation results of the chemical yield and the reaction quantum yield for a range of values of absorbed light power are shown in Figure 5. The slight kinks in the traces of Figure 5a) are due to a change in propagation step size needed for numerical stability in the total process that covers the time scale from µs to many hours. Obviously, Φ_{tot} is a function of time; the value rises to its maximum before beginning its slow decay. In addition, the behavior of Φ_{tot} as a function of absorbed light power is also quite significant, as the value of Φ_{tot} decreases rapidly with increasing P_{irr}.

The simulation reproduces the experimental findings shown in Figure 3 nearly quantitatively. All significant effects are very well reproduced. We also compare the light power dependence of the maximum quantum yield as determined from the model to the experimental values in Figure 3 and have a perfect agreement. It would be highly unlikely that a multidimensional situation of such high complexity can be represented by a model based on experimental observables and known individual second order rates too such high quality if it would not mirror the underlying mechanisms well. We therefore consider it strong proof of the model sketched in Scheme 2. This

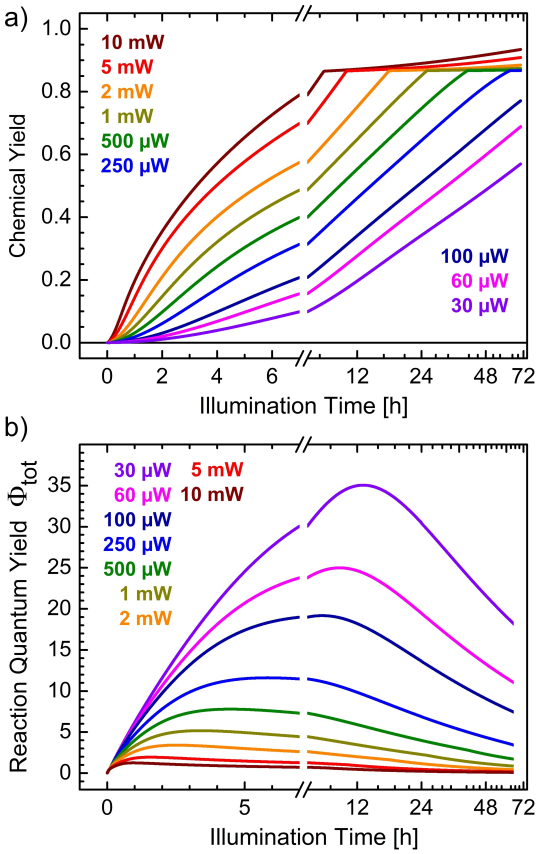

Figure 5. Simulation of the chemical yield and the reaction quantum yield F_{tot} for varying values of the incident light power. a) Time and light power dependent chemical yield of the α-alkylation reaction. b) F_{tot} at various incident light powers.

includes two competing scenarios that depend on the light power and are linked by the key radical **Mal•**: (i) At low incident light powers, one observes a comparatively slow conversion to the reaction product with simultaneously very high Φ_{tot} and Φ_{max}. This suggests that at low concentrations of the excited **Ru** species, the radical chain propagation proceeds via the radical **Mal•** but does not operate very effectively with respect to the formation of the product **DOM**, i.e. the radical chain either proceeds slowly, breaks off again rather quickly (short radical chains), or the photoinduced initiation cycle does not form

Table 2. Summary of the rate constants for the simulation of a-alkylation product formation dynamics. The values shown in the second and fifth row are taken from the literature or preliminary estimates. The optimized values used for the final simulation are shown in rows three and six.

Rate constant	k_1	k_{-1}	k_2	k_3	k_4	k_5
Value $[M^{-1}s^{-1}]$	$K_{eq} = k_1/k_{-1}$ 8×10^{-4}	0.1	1.1×10^6 s^{-1} [49] 1×10^6 s^{-1}	1.1×10^7 [30] 1×10^7	2.7×10^7 [50] 2.7×10^7	$k_3 \ll k_5 \leq 8.3 \times 10^9$ [a] 1×10^8
Rate constant	k_6		k_7	k_8	k_{-8}	k_9
Value $[M^{-1}s^{-1}]$	$\leq k_7 \times 10^{-11}$ ≈ 0.08		$\leq 8.3 \times 10^9$ [a] 8×10^9	$K_P = k_8/k_{-8} = 3.0$ $k_{-8} < k_8$ [b] 1	≈ 0.3	$k_9/k_5 \ll 4 \times 10^{-3}$ M $\approx 10^3$ s^{-1}

[a] Diffusion limited rate constant.[47] [b] Ref. [48].

effectively the radical **MaI**•. (ii) A higher supply of photons increases the concentration of the excited **Ru** species. Experimentally, it is observed that this provides high yields of the product **DOM**, but the photons are used less efficiently (lower Φ_{tot} and Φ_{max}).

As a benefit we can extract the temporal profile of the **MaI**• concentration from the calculation (see Figure 6). The maximum concentration in the sub-nM regime is confirmed. The concentration is highly time and illumination dependent in accord with the observed behavior of the reaction quantum yield. The maximum for each illumination power scales nearly linearly with the optical power. However, the appearance time of the peak increases from below 1 hour to 11 hours for decreasing light level. This matches the increase in chemical yield as seen in Figure 3 a) and also the temporal shift of the maximum of Φ_{diff} (Figure 3 d)).

The efficient conversion to the product **DOM** cannot be simply explained by the radical chain propagation, because this operates effectively with respect to the consumed photons but ineffectively with respect to the formed product **DOM**. There must be another and faster pathway to the reaction product with increasing illumination power (i.e. a higher concentration of excited **Ru** species), which is the closed photoredox catalytic cycle that also produces the key radical **MaI**•. This situation is not reflected in the mechanism postulated by Yoon et al.,[30] since according to their mechanism the radical chain is only started by the photoinduced initiation process and subsequently operates independently of light by radical chain propagation. In this case, a higher radiation power would generate more of the radical **MaI**•, which, according to this mechanism, would maintain the radical chain propagation. Accordingly, Φ_{tot} would not alter with the illumination power.

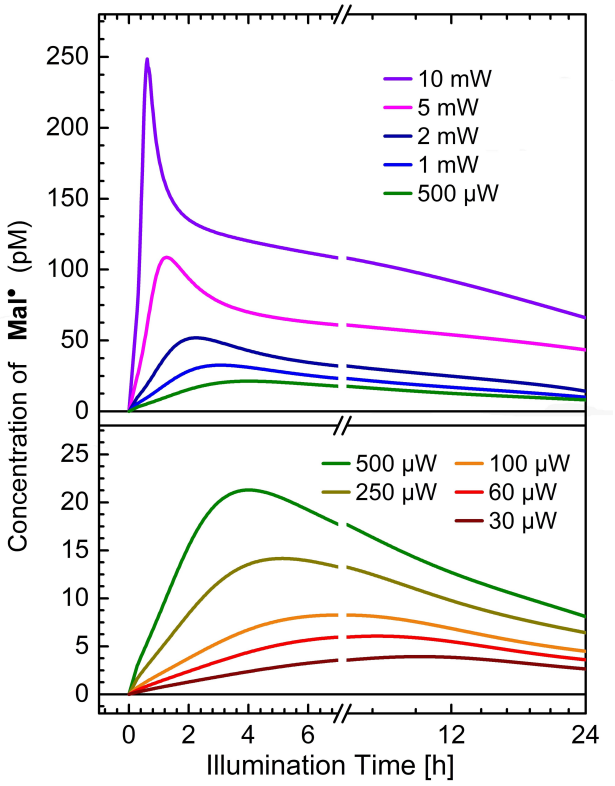

Figure 6. Simulated temporal evolution of [**MaI**•] for various illumination levels.

3. Conclusions

In conclusion, this study makes clear that the accurate determination of the reaction quantum yield is a highly desirable method to normalize and reference the performance of different photocatalysts and reactions. Even though a new visible-light actinometry was recently developed by Scaiano *et al.* to study $[Ru(bpy)_3]Cl_2$-mediated photoredox catalytic transformations[45] the direct measurement of the reaction quantum yields during the time course of such photocatalytic reactions has significant advantages. Our opto-electronic device allows the rapid and facile determination of absolute reaction quantum yields in a typical organic-chemistry laboratory because the device determines the light input, and the absorbed amount of light, and thereby discriminates between productive and incident photons. This direct determination of the reaction quantum yield for the selected model reaction revealed that this parameter cannot be regarded as a single, isolated value but must be considered as a function of both irradiation time and incident light power. Reported values of the reaction quantum yield for this reaction range from $\Phi_{tot} =$ 0.49 to 18 and hence represent only single snapshots at given irradiation times and light input. Most importantly, we found out that the power of the light energy decides about the mechanism of the photocatalytic reaction. In particular, the light power influences the competition between an open shell, chain propagation mechanism (predominant at incident light powers lower than 1 mW) and a closed shell, photoredox catalytic cycle mechanism. These results are of fundamental importance for the current debate about the mechanistic scenarios of photoredox catalytic reactions.

Acknowledgements

Financial support of this work by Deutsche Forschungsgemeinschaft through the GRK 1626 and the SFB 749 is gratefully acknowledged. Open access funding enabled and organized by Projekt DEAL.

Conflict of Interest

The authors declare no conflict of interest.

Keywords: actinometry · light power · organocatalysis · quantum yield · radical chain

[1] M. H. Shaw, J. Twilton, D. W. C. MacMillan, *J. Org. Chem.* **2016**, *81*, 6898–6926.

[2] a) L. Marzo, S. K. Paigre, O. Reiser, B. König, *Angew. Chem. Int. Ed.* **2018**, *57*, 10034–10072; *Angew. Chem.* **2018**, *130*, 10188–10228; b) N. A. Romero, D. A. Nicewicz, *Chem. Rev.* **2016**, *116*, 10075–10166.
[3] K. L. Skubi, T. R. Blum, T. P. Yoon, *Chem. Rev.* **2016**, *116*, 10035–10074.
[4] D. Staveness, I. Bosque, C. R. J. Stephenson, *Acc. Chem. Res.* **2016**, *49*, 2295–2306.
[5] L. Buzzetti, G. E. M. Crisenza, P. Melchiorre, *Angew. Chem. Int. Ed.* **2019**, *58*, 3730–3747; *Angew. Chem.* **2019**, *131*, 3768–3786.
[6] E. Meggers, *Chem. Commun.* **2015**, *51*, 3290–3301.
[7] Y.-Q. Zou, F. M. Hörmann, T. Bach, *Chem. Soc. Rev.* **2017**, *47*, 278–290.
[8] D. M. Arias-Rotondo, J. K. McCusker, *Chem. Soc. Rev.* **2016**, *45*, 5803.
[9] M. Oelgemöller, N. Hoffmann, *Org. Biomol. Chem.* **2016**, *14*, 7392–7442.
[10] S. Fukuzumi, K. Ohkubo, *Org. Biomol. Chem.* **2014**, *12*, 6059–6071.
[11] D. Ravelli, M. Fagnoni, A. Albini, *Chem. Soc. Rev.* **2013**, *42*, 97–113.
[12] K. Zeitler, M. Neumann, in: *Chemical Photocatalysis*, 2nd ed., B. König (ed.), De Gruyter, Berlin, **2020**, pp. 245–284.
[13] A. Pannwitz, O. S. Wenger, *Chem. Commun.* **2019**, *55*, 4004–4014.
[14] M. Majek, A. Jacobi von Wangelin, *Acc. Chem. Res.* **2016**, *49*, 2316–2327.
[15] M. N. Hopkinson, A. Tlahuext-Aca, F. Glorius, *Acc. Chem. Res.* **2016**, *49*, 2261–2272.
[16] Q.-Q. Zhou, Y.-Q. Zou, L.-Q. Lu, W.-J. Xiao, *Angew. Chem. Int. Ed.* **2019**, *58*, 1586–1604; *Angew. Chem.* **2019**, *131*, 1600–1619.
[17] C.-S. Wang, P. H. Dixneuf, J.-F. Soulé, *Chem. Rev.* **2018**, *118*, 7532–7585.
[18] M. Parasram, V. Gevorgyan, *Chem. Soc. Rev.* **2017**, *46*, 6227–6240.
[19] M. Reckenthäler, A. G. Griesbeck, *Adv. Synth. Catal.* **2013**, *355*, 2727–2744.
[20] J. W. Tucker, C. R. J. Stephenson, *J. Org. Chem.* **2012**, *77*, 1617–1622.
[21] B. König, S. Kümmel, E. Svobodvá, R. Cibulka, in: *Chemical Photocatalysis*, 2nd ed., B. König (ed.), De Gruyter, Berlin, **2020**, pp. 45–71.
[22] U. Megerle, M. Wenninger, R.-J. Kutta, R. Lechner, B. König, B. Dick, E. Riedle, *Phys. Chem. Chem. Phys.* **2011**, *13*, 8869–8880.
[23] I. Ghosh, L. Marzo, A. Das, R. Shaikh, B. König, *Acc. Chem. Res.* **2016**, *49*, 1566–1577.
[24] J. B. McManus, D. A. Nicewicz, *J. Am. Chem. Soc.* **2017**, *139*, 2880–2883.
[25] E. Speckmeier, T. G. Fischer, K. Zeitler, *J. Am. Chem. Soc.* **2018**, *140*, 15353–15365.
[26] F. Speck, D. Rombach, H.-A. Wagenknecht, *Beilstein J. Org. Chem.* **2019**, *15*, 52–59.
[27] D. A. Nicewicz, T. M. Nguyen, *ACS Catal.* **2014**, *4*, 355–360.
[28] J. K. Sideri, E. Voutyritsa, C. G. Kokotos, *Org. Biomol. Chem.* **2018**, *16*, 4596–4614.
[29] H. J. Kuhn, S. E. Braslavsky, R. Schmidt, *Pure Appl. Chem.* **2004**, *76*, 2105–2146.
[30] M. A. Cismesia, T. P. Yoon, *Chem. Sci.* **2015**, *6*, 5426–5434.
[31] M. D. Kärkäs, B. S. Matsuura, C. R. J. Stephenson, *Science* **2015**, *349*, 1285–1286.
[32] U. Megerle, R. Lechner, B. König, E. Riedle, *Photochem. Photobiol. Sci.* **2010**, 9, 1400–1406.
[33] IUPAC. Compendium of Chemical Terminology, 2nd ed. (the "Gold Book"). Compiled by A. D. McNaught, A. Wilkinson. Blackwell Scientific Publications, Oxford (1997). Online version (2019-) created by S. J. Chalk. ISBN 0-9678550-9-8. https://goldbook.iupac.org/terms/view/Q04991.
[34] D. A. Nicewicz, D. W. C. MacMillan, *Science* **2008**, *322*, 77–80.
[35] M. Neumann, S. Füldner, B. König, K. Zeitler, *Angew. Chem. Int. Ed.* **2011**, *50*, 951–954; *Angew. Chem.* **2011**, *123*, 981–985.
[36] C. G. Hatchard, C. A. Parker, *Proc. R. Soc. London Ser. A* **1956**, *235*, 518–536.
[37] H. J. Kuhn, S. E. Braslavsky, R. Schmidt, *Pure Appl. Chem.* **2004**, *76*, 2105–2146.
[38] H. Volfova, Q. Hu, E. Riedle, *EPA Newsl.* **2019**, 51–69.
[39] A. Bahamonde, P. Melchiorre, *J. Am. Chem. Soc.* **2016**, *138*, 8019–8030.
[40] S. Eckel, A. O. Sushkov, S. K. Lamoreaux, *Rev. Sci. Instrum.* **2012**, *83*, 026106.
[41] A. K. Bhattacharya, N. R. Dhar, *Z. Anorg. Allg. Chem.* **1928**, *175*, 357–366.
[42] M. Bodenstein, H. Lütkemeyer, *Z. Phys. Chem.* **1924**, *114*, 208–236.
[43] O. Rice, *J. Chem. Phys.* **1942**, *10*, 440–444.
[44] A. Shepp, *J. Chem. Phys.* **1956**, *24*, 939–943.
[45] S. P. Pitre, C. D. McTiernan, W. Vine, R. DiPucchio, M. Grenier, J. C. Scaiano, *Sci. Rep.* **2015**, *5*, 16397.
[46] Q. Hu, doctoral thesis at the LMU München (2020), DOI: 10.5282/edoc.26549.
[47] M. Montalti, A. Credi, L. Prodi, M. T. Gandolfi, *Handbook of photochemistry*, CRC press, **2006**.
[48] B. Reiß, doctoral thesis at the Karlsruher Institut für Technologie (2017), DOI: 10.5445/IR/1000074351.
[49] J. V. Caspar, T. J. Meyer, *J. Am. Chem. Soc.* **1983**, *105*, 5583–5590.
[50] S. Campagna, F. Puntoriero, F. Nastasi, G. Bergamini, V. Balzani, *Top. Curr. Chem.* **2007**, *280*, 117–214.

Manuscript received: April 20, 2021
Revised manuscript received: June 9, 2021
Accepted manuscript online: June 18, 2021
Version of record online: ■■, ■■■

ARTICLES

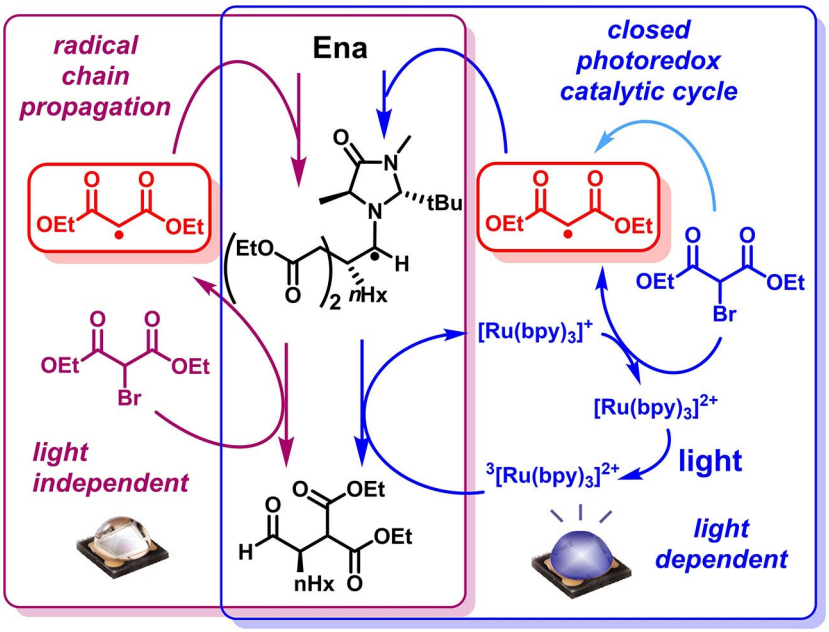

More than 100 % with less light! The power of the light energy significantly influences the mechanism of the photocatalytic reaction. This can be specifically described as a radical chain propagation mechanism with a reaction quantum yield of >1 and a closed photoredox catalytic cycle with a reaction quantum yield of <1.